A density-functional theory for $(BAs)_n$ clusters (n=1–14): structures, stabilities and electronic properties*

Liu Zhi-Feng(刘志锋), Lei Xue-Ling(雷雪玲), Liu Li-Ren(刘立仁), Liu Huo-Yan(刘火雁), and Zhu Heng-Jiang(祝恒江)†

School of Physics and Electronic Engineering, Xinjiang Normal University, Urumchi 830054, *China*

(Received 24 July 2010; revised manuscript received 22 August 2010)

This paper investigates the lowest-energy structures, stabilities and electronic properties of $(BAs)_n$ clusters (n=1–14) by means of the density-functional theory. The results show that the lowest-energy structures undergo a structural change from two-dimensional to three-dimensional when $n = 4$. With the increase of the cluster size ($n \geqslant 6$), the $(BAs)_n$ clusters tend to adopt cage-like structures, which can be considered as being built from B_2As_2 and six-membered rings with B–As bond alternative arrangement. The binding energy per atom, second-order energy differences, vertical electron affinity and vertical ionization potential are calculated and discussed. The caculated HOMO–LUMO gaps reveal that the clusters have typical semiconductor characteristics. The analysis of partial density of states suggests that there are strong covalence and molecular characteristics in the clusters.

Keywords: $(BAs)_n$ clusters, density-functional theory, lowest-energy structures, electronic properties

PACS: 31.15.es **DOI:** 10.1088/1674-1056/20/2/023101

1. Introduction

Clusters, the transitional forms between atoms and nanometer scale structures or bulk, exhibit many interesting properties which are neither atomic-like nor extended solid-like. Moreover, the properties, such as the optical, magnetic and mechanic characteristics, change as the size of the cluster varies. It is expected that materials assembled from finite-sized clusters may have special properties. Thus much attention has been paid to the study of atomic clusters from both theoretical and experimental sides during the recent years.[1−5] For III–V semiconductor clusters, due to their fundamental importance in theory study and potential applications in micro-electronic and optical industry, the clusters like gallium arsenide, gallium nitride and aluminum arsenide etc. have been investigated extensively.[6−15]

As a substantial candidate for the III–V semiconductor, boron arsenide, a kind of indirect band gap semiconductor, has resemblance with silicon electronically[16] and is an alternate to gallium nitride as a wide gap partner for alloying with aluminum arsenide and gallium arsenide.[17] According to the Phillips's scale of electronegativities,[18,19] boron is more electronegative than arsenic. Tight-binding calculation[20] has pointed out that the effective charges of boron arsenide are negative, which is opposite to other zinc-blende semiconductor. These peculiar behaviours of boron arsenide inspired research interests both on experimental and theoretical sides[21−26] in its bulk state. For instance, Meradji *et al.*[22] have investigated the elastic constants and electronic structure of boron arsenide using the first-principles total-energy computation with local density approximation (LDA) and general gradient approximation (GGA). Wentzcovitch *et al.*[23−25] calculated the relative stabilities of boron arsenide at high pressures by the total-energy pseudopotential technique. Ahmed *et al.*[26] have studied the theoretical lattice parameters, bulk modulus and electronic band structure of boron arsenide with LDA and GGA as well

*Project supported by the National Natural Science Foundation of China (Grant No. 10964012), the Priority Subject Program for Theoretical Physics of Xinjiang Normal University and the Fund of the Education Department of Xinjiang Uygur Autonomous Region of China (Grant No. xjedu2009i27) and the Science and Technology Innovation Foundation for Graduate Students of Xinjiang Normal University (Grant No. 20101205).

†Corresponding author. E-mail: zhj@xjnu.edu.cn

© 2011 Chinese Physical Society and IOP Publishing Ltd

as GGA–proposed by Engel and Vosko. Although boron arsenide has been studied extensively in its bulk state, investigations in cluster phase have been rarely reported yet.[27]

In our previous work, the structural and electronic properties of boron or boride clusters[28−31] have been investigated by the density-functional theory (DFT). In this paper, based on the previous studies, the results of a systematic theoretical study on the $(BAs)_n$ clusters (n=1–14) are presented by using the DFT, selecting Becke's non-local three-parameter hybrid functional combined with the Lee–Yang–Parr correlation (B3LYP) method by means of efficient gradient techniques with the 6-31+G(d) basis set. The main focus of this work is to analyse the structures, stabilities and electronic properties of these clusters, and the aim of all these studies is to answer the following questions. Firstly, which structure would be the lowest-energy structure for each cluster size? Are there any laws of the structures' growth? Secondly, who is the most stable cluster for $(BAs)_n$? How does the binding energy change with the increasing cluster size? Thirdly, how are the electronic properties in the clusters, such as vertical ionization potential (VIP), vertical electron affinity (VEA) and HOMO–LUMO (highest occupied molecular orbital–lowest unoccupied molecular orbital) gaps? What kind of bonds is formed between B atoms and As atoms in the $(BAs)_n$ clusters?

This paper is organized as follows. In Section 2, we describe the computational details in brief. In Section 3 we present the lowest energy structures of $(BAs)_n$ clusters (n=1–14) and discuss their growth behaviour. The relative stability and electronic properties of these clusters are also discussed. Finally, the conclusions are given in Section 4.

2. Computational details

The selection of distinct initial geometries is important to the reliability of the obtained ground state structures. As the increase of cluster size, the number of the possible geometries increases dramatically. For each initial structure, previous studies of III–V compound clusters [6−15,32] are seen as a guide, and all possible $(BAs)_n$ clusters including arbitrary construction are considered. The geometries with different symmetries are also optimized for each size. The stabilities of $(BAs)_n$ (n=1–14) are examined by evaluating the harmonic frequencies. For each of these clusters, all computed frequencies are confirmed as real.

All calculations are based on DFT in the GAUSSIAN-03 package. In the electronic structure calculations, the B3LYP method with 6-31+G(d) basis sets have been chosen. Self-consistent field calculations are done with a convergence criterion of 10^{-6} Hartree on the total energy. In the geometrical optimization, the convergence thresholds are set to 0.00045 a.u./Bohr for the maximum force, 0.0018 a.u. for the maximum displacement, and 10^{-5} Hartree for the energy change.

In order to test the quality of the scheme for the description of $(BAs)_n$ (n=1–14) clusters, we first consider B_2 and As_2 for which experimental data are available for comparison. For boron dimer the bond length of 0.1620 nm and the vibrational frequency of 1004.44 cm^{-1} are consistent with the earlier DFT results[33] and the experimental values of 0.1590 nm and 1051.30 cm^{-1}.[34,35] The bond length of the arsenic dimer is obtained as 0.2103 nm, which agrees well with the experimental values of 0.2103 nm,[36] the computed vibrational frequency of 435.8 cm^{-1} is well-reproduced in comparison with the experimental value of 430.0 cm^{-1}.[36] The As_4 tetramer was also calculated by the same method. The results show that tetrahedron is the most stable structure, and the As–As bond length and vibrational frequency are 0.2444 nm and 200.2 cm^{-1}, 254.7 cm^{-1}, 347.2 cm^{-1}, respectively. This result is in good agreement with the experimental values of 0.2435 nm[37] and 200.8 cm^{-1}, 251.0 cm^{-1}, 342.0 cm^{-1}.[38] Therefore, we have confidence to use the same basis set throughout the whole calculation.

3. Results and discussion

3.1. Lowest-energy structures and growth path

Using the computation scheme described in Section 2, we have explored a number of low-lying isomers and determined the lowest-energy structures for $(BAs)_n$ (n=1–14) clusters. Only the lowest-energy structures are shown in Figs. 1 and 2. Their bond lengths of B–As, B–As–B angles and the lowest vibrational frequencies are given in Table 1. The lowest vibrational frequencies can reflect whether the imaginary frequency exists or not. It is found that all the

frequencies are positive; therefore, the optimized geometry with the lowest energy is located at the minimum point of the potential surface.

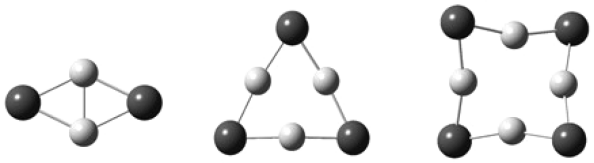
In order to show the lowest-energy structures in a more understandable way, we have divided these clusters into two groups according to the structural characteristics. In group 1, $(BAs)_n$ clusters (n=2–4) are included whose geometries are planar or near-planar ring-like structures. In group 2, the rest of the clusters are included for which the geometries are cage-like structures.

The lowest-energy structures of the clusters in group 1 have been seen to be planar rings (n=2–3) or near-planar ring (n = 4). The main reason to break the planarity in the ring structures is the observed strong tendency to form larger B–As–B angles. Additionally, the bond lengths of B–As are shortened as the size of the ring increases.

Table 1. The B–As bond lengths, B–As–B angles and the lowest vibrational frequencies (LVF) of the lowest-energy structures for $(BAs)_n$ clusters (n=1–14).

cluster	B–As/nm	θ B–As–B/(°)	LVF/cm^{-1}
BAs	0.1751		952.2
B_2As_2	0.1936	52.36	295.9
	0.1952[27]	52.3[27]	
B_3As_3	0.1911	61.82	104.6
B_4As_4	0.1890	65.72	36.5
B_5As_5	0.2059	65.53–97.52	108.1
B_6As_6	0.2032	68.25–92.42	100.7
B_7As_7	0.2031	65.99–99.72	96.6
B_8As_8	0.2024	64.42–103.52	61.3
B_9As_9	0.1955	70.54–103.89	73.4
$B_{10}As_{10}$	0.2022	64.82–105.29	69.6
$B_{11}As_{11}$	0.2013	67.57–105.31	58.9
$B_{12}As_{12}$	0.2007	74.81–100.36	91.2
$B_{13}As_{13}$	0.2013	66.00–119.91	73.3
$B_{14}As_{14}$	0.2007	73.01–123.50	28.3
crystal	0.4777[39]		

For B_2As_2, the lowest-energy structure is the rhombus with D_{2h} symmetry. The bond lengths of B–B and B–As are 0.1558 nm and 0.1820 nm, respectively. The As–B–As angle is 127.6° in the structure. These results are consistent with the previous theoretical study.[27] The isovalent Al_2As_2 was investigated by Guo[32] using the same method and thus, comparison of them is warranted. For the rhombus Al_2As_2 structure, the optimized As–As and Al–As bond lengths and Al–As–Al angle are 0.2308 nm, 0.2660 nm and 128.6°, respectively. The B–As bond lengths is shorter than that of Al–As, and the B–As–B angle is less than that of Al–As–Al, implying that there are stronger B–As and B–B bonding in the cluster for B_2As_2. For B_3As_3, the lowest-energy structure is planar six-membered ring (6MR) with C_s symmetry. It presents alternate boron and arsenic atoms, with three arsenic atoms edge-capping the triangle formed by boron atoms. For B_4As_4, the most stable configuration is near-planar eight-membered ring with S_4 symmetry, which can be looked as the transition between planar and three-dimensional structures. It also presents alternate boron and arsenic atoms, with the four arsenic atoms edge-capping the quadrangle formed by boron atoms.



B_2As_2 D_{2h} B_3As_3 C_s B_4As_4 S_4

Fig. 1. The lowest-energy structures of $(BAs)_n$ (n=2–4) clusters. Arsenic atoms are represented by the dark spheres and boron atoms are represented by the light spheres.

The group 2 contains the $(BAs)_n$ clusters (n=5–14) whose lowest-energy structures are cage-like. For B_5As_5, four B_2As_2 clusters and two 6MR units can be found in the structure. The same building blocks can also be found in the most stable configuration of B_6As_6, which is built from two parallel 6MR units joined together by six B_2As_2 units. For B_7As_7, there is a B–As capping on one of surfaces of B_6As_6 polyhedron. The lowest-energy structure of B_8As_8 is also built by B_2As_2 and 6MR units. It may be viewed as a four-faced polyhedron where each face is built by B_2As_2 and 6MR, which are rotated in order to build the next face. This structure has B_2As_2 rings at the top and bottom. Altogether, six rhombi and four hexagons are found in this structure. For B_9As_9, the most stable configuration is cage-like structure composed of B_2As_2 and 6MRs. These 6MRs may be envisioned as caps of a polyhedron joined by a ring formed of B_2As_2 and 6MR units. The ring is constructed with alternating one 6MR unit and two joined B_2As_2 units. There are six rhombi and five hexagons in this structure, which has C_{3h} symmetry. The structure of $B_{10}As_{10}$ is ellipsoid, which can be deemed as the combination of two B_6As_6 units with some common atoms. For $B_{11}As_{11}$, six B_2As_2 and seven 6MRs

can be found in its lowest-energy structure. As for $B_{12}As_{12}$, a fullerene-like cage with high symmetry S_6 is the lowest-energy structure. And our following analysis of binding energy per atom, second-order energy differences and HOMO–LUMO gaps show that it is the most stable cluster of $(BAs)_n$ (n=1–14). It is expected that the most stable cluster will be one of the practical nano structured material units. We hope that the further experimental approval will be carried out. For $B_{13}As_{13}$, the most stable configuration is composed of three B_6As_6 clusters with some mutual atoms, and six rhombi and nine hexagons can be found in the structure with C_{3v} symmetry. The lowest-energy structure of $B_{14}As_{14}$ is built from $B_{13}As_{13}$ by capping a B–As bond on one of the polyhedron surfaces.

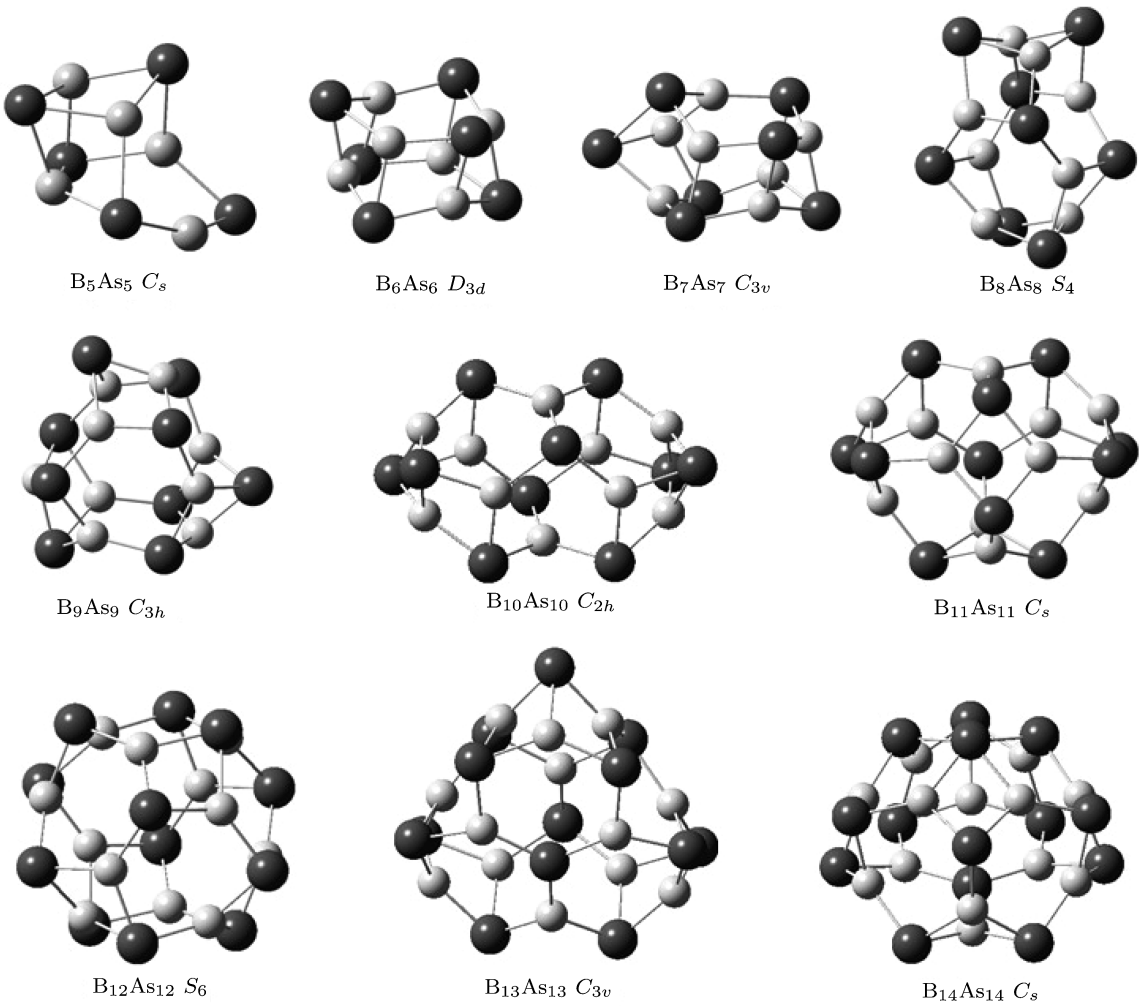


Fig. 2. The lowest-energy structures of $(BAs)_n$ (n=5–14) clusters. Arsenic atoms are represented by the dark spheres and boron atoms are represented by the light spheres.

From the above discussion, there are two basic building blocks found in the construction of the lowest-energy structures, i.e. B_2As_2 and 6MR with B–As bond alternative arrangement. For example, two 6MRs can be found in B_5As_5, B_6As_6 and B_7As_7. As the increase of the cluster size, four, five, six, seven, eight, nine and ten 6MRs are found in B_8As_8, B_9As_9, $B_{10}As_{10}$, $B_{11}As_{11}$, $B_{12}As_{12}$, $B_{13}As_{13}$ and $B_{14}As_{14}$, respectively. It is noteworthy that the zinc-blend structure of boron arsenide crystal can be constructed by the same type of B–As 6MRs. Thus, the lowest-energy structure consisting of 6MRs with B–As alternative arrangement can be viewed as the embryo of zinc-blende structure of boron arsenide crystal. Moreover, because of the intensive direction-properties of the B–As covalent bond (the bond covalency can be concluded by analysing the partial density of state (PDOS) for the clusters), there is not radical change in the structures for $(BAs)_n$ clusters (n=6–14).

3.2. Sized dependence of cluster properties

An unambiguous insight into the relative stability of $(BAs)_n$ clusters can be obtained by analysing their energies. We firstly calculate the binding energy per atom, E_b, which is defined as

$$E_b = \frac{nE(B) + nE(As) - E[(BAs)_n]}{2n}, \quad (1)$$

where $E[(BAs)_n]$ is the lowest energy of the structure for $(BAs)_n$ cluster, $E(B)$ and $E(As)$ are the energies of the boron and arsenic atoms, respectively. The binding energy per atom for $(BAs)_n$ clusters versus the number of BAs units are displayed in Fig. 3. As seen in this figure, except for the case of n=13, the binding energy per atom increases monotonically as the size of clusters increases, implying that the clusters can continue to gain energy during the growth. That is to say, this system may form a greater size cluster. It also suggests that the energy convergence to bulk behaviour is slow in these small clusters, which can be testified by the analysis of PDOS (shown in our following discussion). Furthermore, the slope of the curve in Fig. 3 is large for the small cluster sizes, whereas starting from $n = 4$ the curve is almost flat with a slight slope. We have known that from $n = 5$ to 14, the number of 6MR units in the lowest-energy structure increases gradually. It indicates that the increase of 6MR units in the lowest-energy structure is helpful to enhance the stability of the clusters. Though, the curve tends to be flat, a local peak can be found at $n = 12$, which shows that $B_{12}As_{12}$ is more stable than its neighbours.

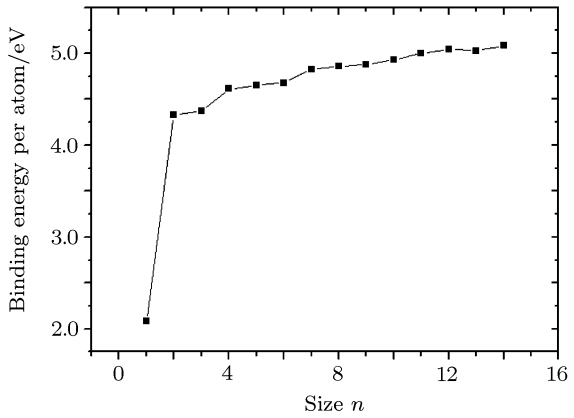


Fig. 3. The binding energy per atom of $(BAs)_n$ (n=1–14) clusters as a function of cluster size n.

In Fig. 4, we present the second-order difference of total energy for the $(BAs)_n$ clusters, which is defined by

$$\Delta_2 E(n) = E(n-1) + E(n+1) - 2E(n), \quad (2)$$

where $E(n-1)$, $E(n+1)$ and $E(n)$ represent the total energy of the lowest energy structure $(BAs)_{n-1}$, $(BAs)_{n+1}$ and $(BAs)_n$ clusters, respectively. In cluster physics, the second-order energy difference is a sensitive quantity that reflects the relative stability of cluster and can be directly compared with the experimental relative abundance. As shown in Fig. 4, the values of magic number of $(BAs)_n$ clusters are found to be 4, 7 and 12, implying that these clusters are more stable than their neighbouring clusters. Moreover, the value of $\Delta_2 E$ has an evident peak for $n = 12$, namely $B_{12}As_{12}$ is the most stable cluster. For $B_{12}As_{12}$, the lowest-energy structure is the fullerene-like cage with high symmetry S_6, a high number of hexagons as building blocks. The atomic structure effect may enhance the stability of $B_{12}As_{12}$ cluster. These results are consistent with previous studies[32] of isovalent $Al_{12}As_{12}$ cluster.

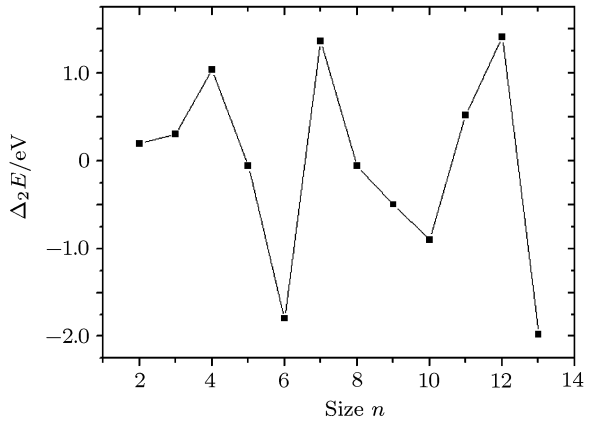


Fig. 4. The second-order energy difference $\Delta_2 E$ of the $(BAs)_n$ (n=1–14) clusters as a function of cluster size n.

The energy difference between the HOMO and LUMO reflects the ability for electrons to jump from occupied orbital to unoccupied orbital and represents the ability for the molecular orbital to participate the chemical reactions to some extent. A larger HOMO–LUMO gap corresponds to a weaker chemical activity. From Fig. 5, it is observed that there is an increasing tendency for the gap when the cluster size increases, namely, there is a decreasing tendency of the chemical activity during the increase of cluster size. It is worthy to point out that HOMO–LUMO gap is also considered as an important parameter to estimate the electronic stability of a small cluster. The larger energy gap indicates more electronic stability. In Fig. 5, the highest peak of HOMO–LUMO gaps appear at the

size of 12, implying that $B_{12}As_{12}$ possesses the highest electronic stability, which accords with the analysis of E_b and $\Delta_2 E$. Furthermore, the semiconductor-like properties can also be found in the clusters by calculating of HOMO–LUMO gap, which shows that the value of the gap varies from 0.7075 eV to 3.2379 eV.

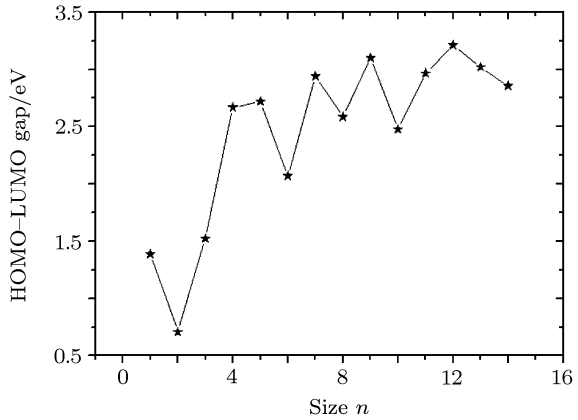


Fig. 5. The HOMO–LUMO gaps of the $(BAs)_n$ (n=1–14) clusters against the cluster size.

Other sensitive quantities to provide fundamental insight into the electronic structure and chemical reactivity with other molecules are the ionization potentials and electron affinities of the clusters. Therefore, we have calculated the VIP and VEA of $(BAs)_n$ (n=1–14) clusters. The VIP and VEA are calculated with the following definitions:

$$\begin{aligned} \mathrm{VIP} &= E[\text{nonoptimized}(BAs)_n{}^+] \\ &\quad - E[\text{optimized}(BAs)_n], \qquad (3) \\ \mathrm{VEA} &= E[\text{optimized}(BAs)_n] \\ &\quad - E[\text{nonoptimized}(BAs)_n{}^-]. \qquad (4) \end{aligned}$$

As shown in Figs. 6 and 7, it is obvious that a decreasing tendency can be seen when the number of BAs units increases for both VIP and VEA. The same tendency can be found by the previous study of its isovalent $(AlAs)_n$ (n=1–14).[32] It is known that the larger VIP value is, the stronger nonmetallic characteristic will be, and the larger VEA is, the stronger metallic characteristic is. So the decreases for both VIP and VEA indicate that both the clusters' nonmetallic and metallic characteristics become weak. That is to say, certain covalence exists in the clusters. Moreover, particular large values for VIP are exhibited with n = 1, 4, 9, 12 in Fig. 6. The VIP of analogues, namely $(AlAs)_n$ (n=1–14) were studied by Guo.[32] It is interesting to compare the calculated results. The particular large VIP values of the $(AlAs)_n$ (n=1–14) are exhibited with n=1, 6, 12. In the case of VEA, the particular small values appear at n=5, 7, 9, 12, while n=2, 9, 12 for $(AlAs)_n$ (n=1–14).

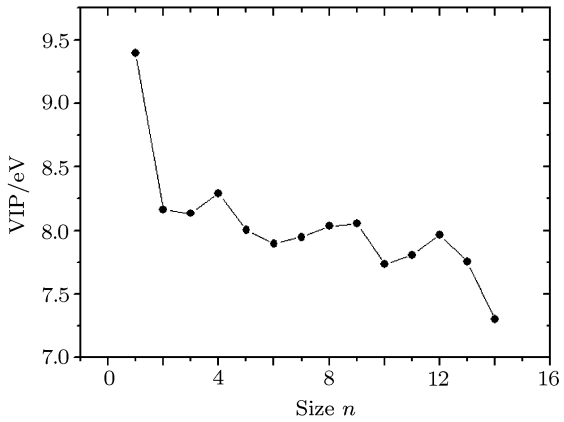


Fig. 6. Sized dependence of VIP for the $(BAs)_n$ (n=1–14) clusters.

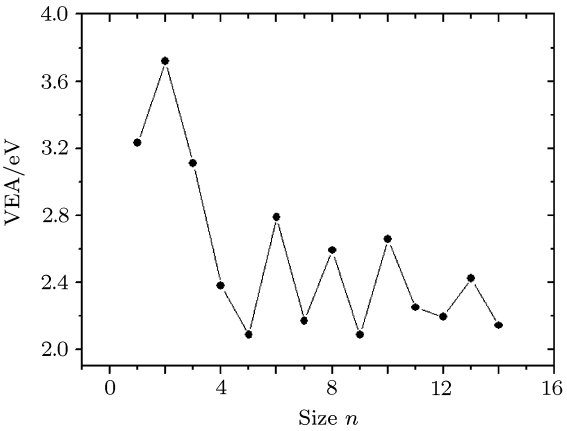


Fig. 7. Sized dependence of VEA for the $(BAs)_n$ (n=1–14) clusters.

To obtain fundamental understanding of the bonding behaviour of $(BAs)_n$ (n=1–14) clusters, we calculate the PDOS of the clusters (shown in Fig. 8). For each cluster the PDOS is plotted as a function of the energy. In plotting the PDOS each discrete energy level is replaced by a Lorentzian with full width at half maximum given by 0.01 eV. As shown in the figure, the PDOS on the Fermi surface comes mainly from the contribution of 4p orbital of arsenic atoms. Moreover, a distinct spd hybrid can be observed at the vicinity of Fermi level. In Fig. 8, for all the clusters the shapes of PDOS are like sharp ridge, indicating that the band character has not appeared, i.e. the energy convergence to bulk behaviour is slow in these small clusters. That is to say, there is strong molecular characteristic for the clusters, because of only 2–28 atoms. The wide pseudo gap is the energy difference between the two corresponding values of the pinnacles which are close to the Fermi level, and the larger wide pseudo gap is, the stronger covalent characteristic will be. So the PDOS of $(BAs)_n$ reveals that there are strong covalent characteristic in the clusters.

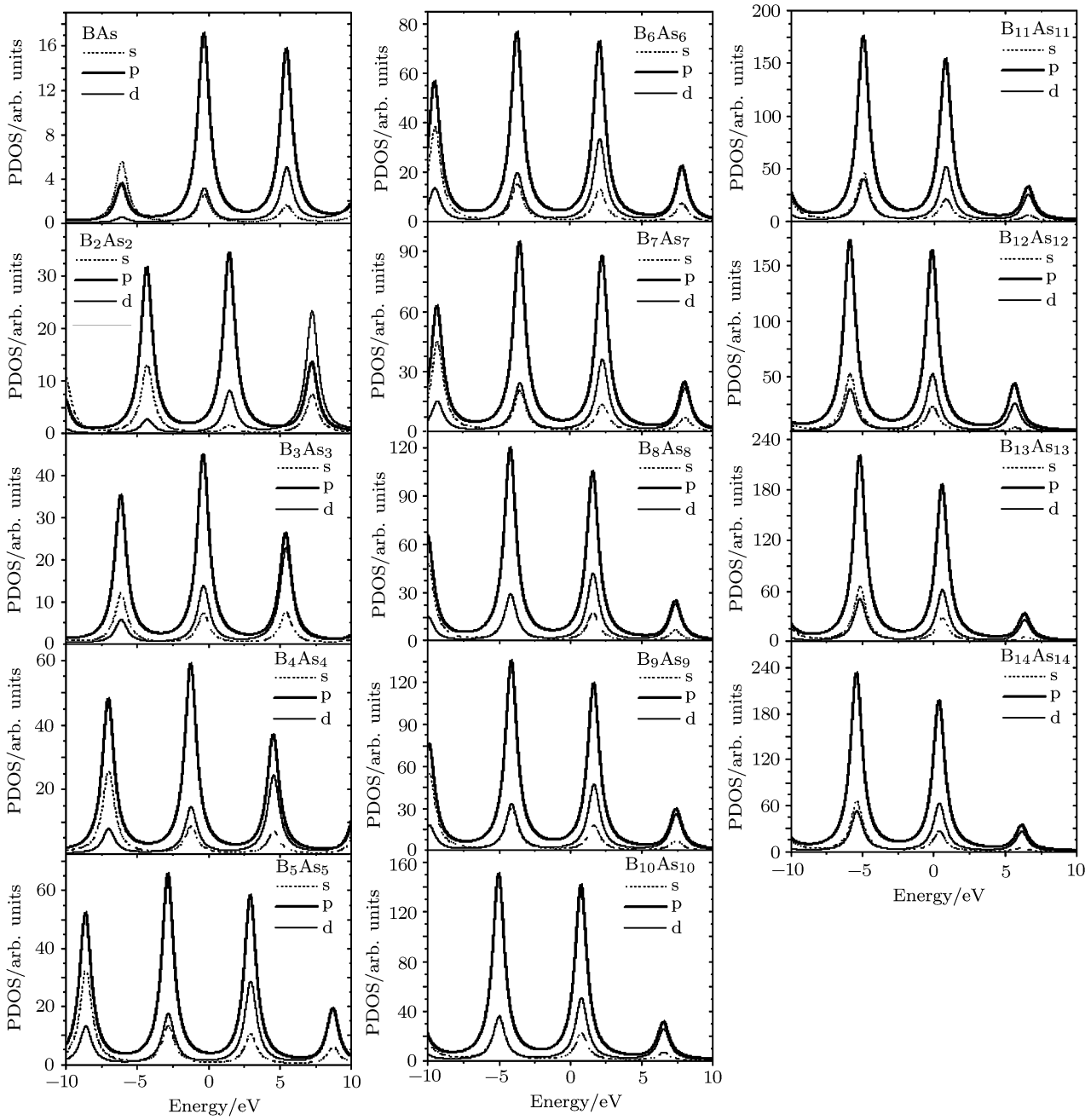


Fig. 8. The PDOS of the $(BAs)_n$ (n=1–14) clusters. The Fermi energy is located at $E = 0$ eV.

4. Conclusions

The first-principles calculations are performed to study the structures, stabilities and electronic properties of the $(BAs)_n$ (n=1–14) clusters. The lowest-energy structures, E_b, $\Delta_2 E$, HOMO–LUMO gaps, VIP, VEA and PDOS of the clusters are presented and discussed. The following conclusions can be drawn: (i) The lowest-energy structures of $(BAs)_n$ clusters undergo a structural change from two-dimensional to three-dimensional at $n = 4$; (ii) The medium size clusters (n=6–14) display cage-like structures, which can be regarded as being built from the blocks of B_2As_2 and 6MRs with B–As bond alternative arrangement; (iii) The analysis of E_b , $\Delta_2 E$ and HOMO–LUMO gaps show that $B_{12}As_{12}$ is the most stable cluster for $(BAs)_n$ (n=1–14); (iv) The results of PDOS analysis reveal that a distinct spd hybrid can be found at the vicinity of Fermi level, and there are strong molecular and covalent characteristic in the clusters.

References

[1] Deshpande M D, Roy S and Kanhere D G 2007 *Phys. Rev.* B **76** 195423

[2] Chen X F, Zhang Y, Qi K T, Li B, Zhu Z H and Sheng Y 2010 *Chin. Phys.* B **19** 033601

[3] Tian F Y, Jing Q and Wang Y X 2008 *Phys. Rev.* A **77** 013202

[4] Lei X L, Zhu H J, Wang X M and Luo Y H 2008 *Chin. Phys.* B **17** 3687

[5] Rahane A, Deshpande M and Pandey R 2010 *J. Nanopart. Res.* **12** 727

[6] Sun L Z, Chen X S, Zhou X H, Sun Y L, Quan Z J and Lu W 2005 *Euro. Phys. J.* D **34** 47

[7] Korambath P P and Karna S P 2000 *J. Phys. Chem.* A **104** 4801

[8] Seeburrun N, Gohee P, Abdallah H H, Kanime L, Archibong E F and Ramasami P 2009 *Chem. Phys. Lett.* **472** 35

[9] Zhao W, Cao P L and Duan W H 2006 *Phys. Lett.* A **349** 224

[10] Kandalam A K, Blanco M A and Pandey R 2002 *J. Phys. Chem.* B **106** 1945

[11] Zhao J J, Wang B L, Zhou X L, Chen X S and Lu W 2006 *Chem. Phys. Lett.* **422** 170

[12] Costales A and Pandey R 2003 *J. Phys. Chem.* A **107** 191

[13] Costales A, Kandalam A K, Franco R and Pandey R 2002 *J. Phys. Chem.* B **106** 1940

[14] Qu Y H, Ma W Y, Bian X F, Tang H W and Tian W X 2005 *J. Mol. Graph. Model* **24** 167

[15] Tozzini V, Buda F and Fasolino A 2001 *J. Phys. Chem.* B **105** 12477

[16] Ferhat M, Bouhafs B, Zaoui A and Aourag H 1998 *J. Phys.: Condens. Matter* **10** 7995

[17] Hart G L W and Zunger A 2000 *Phys. Rev.* B **62** 13522

[18] Phillips J C 1973 *Bonds and Bands in Semiconductors* (New York: Academic)

[19] Van Vechten J A and Phillips J C 1970 *Phys. Rev.* B **2** 2160

[20] Harrison W A 1980 *Electronic Structure and the Properties of Solids* (San Francisco: Freeman)

[21] Osugi J, Shimizu K, Tanaka Y and Kadono K 1966 *Rev. Phys. Chem. Jpn.* **36** 54

[22] Meradji H, Drablia S, Ghemid S, Belkhir H, Bouhafs B and Tadjer A 2004 *Phys. Status Solidi* B **241** 2881

[23] Wentzcovitch R M, Chang K J and Cohen M L 1986 *Phys. Rev.* B **34** 1071

[24] Wentzcovitch R M and Cohen M L 1986 *J. Phys.* C: *Solid State Phys.* **19** 6791

[25] Wentzcovitch R M, Cohen M L and Lam P K 1987 *Phys. Rev.* B **36** 6058

[26] Ahmed R, Hashemifar S J, Akbarzadeh H, Ahmed M and Aleem F 2007 *Comput. Mater. Sci.* **39** 580

[27] Burrill S and Grein F 2005 *J. Mol. Struct.: Theochem* **757** 137

[28] Liu L R, Lei X L, Chen H and Zhu H J 2009 *Acta Phys. Sin.* **58** 5355 (in Chinese)

[29] Lei X L, Wang Q L, Yan Y L, Zhao W J, Yang Z and Luo Y H 2007 *Acta Phys. Sin.* **56** 4484 (in Chinese)

[30] Lei X L, Zhu H J, Ge G X, Wang X M and Luo Y H 2008 *Acta Phys. Sin.* **57** 5491 (in Chinese)

[31] Yang Z, Yu Y L, Zhao W Z, Lei X L, Ge G X and Luo Y H 2007 *Acta Phys. Sin.* **56** 2590 (in Chinese)

[32] Guo L 2008 *Comput. Mater. Sci.* **42** 489

[33] Yang C L, Zhu Z H, Wang R and Liu X Y 2001 *J. Mol. Struct.: Theochem* **548** 47

[34] Lide D R 2006 *CRC Handbook of Chemistry and Physics* 87th edn. (New York: CRC Press) p. 82

[35] Rosen B 1970 *Spectroscopic Data Relative to Diatomic Molecules* (Oxford: Pergamon)

[36] Huber K and Herzberg G 1979 *Molecular Spectra and Molecular Structure IV Constants of Diatomic Molecules* (New York: Van Nostrand) p. 504

[37] Bosworth Y M, Clark R J H and Rippon D M 1973 *J. Mol. Spectrosc.* **46** 240

[38] Brumbach S B and Rosenblatt G 1972 *J. Chem. Phys.* **56** 3110

[39] Wyckoff R W G 1986 *Crystal Structures* 2nd edn. (Malabar: Krieger)